Indian Journal of Pure & Applied Physics
Vol. 58, May 2020, pp. 358-362

Investigation of 14.1 MeV neutrons interaction with C, Mg, Cr

N A Fedorov[a,b*], I D Dashkov[a], D N Grozdanov[b,c], Yu N Kopatch[b], I N Ruskov[c], V R Skoy[b], T Yu Tretyakova[d,b], F A Aliev[b,e], S Dabylova[b,f], N A Gundorin[b], C Hramco[b,g] & TANGRA collaboration

[a]Lomonosov Moscow State University, Moscow, Russia

[b]Joint Institute for Nuclear Research, Dubna, Russia

[c]Institute for Nuclear Research and Nuclear Energy of the Bulgarian Academy of Sciences, Sofia, Bulgaria

[d]Skobeltsyn Institute of Nuclear Physics, Lomonosov Moscow State University, Moscow, Russia

[e]Institute of Geology and Geophysics of Azerbaijan, National Academy of Sciences, Baku, Azerbaijan

[f]LN Gumilyov Eurasian National University, Republic of Kazakhstan

[g]Institute of Chemistry of the Academy of Sciences of Moldova, Chisinau, Republic of Moldova

Received 23 March 2020

This paper is dedicated to n+^{12}C, n+^{24}Mg, n+^{52}Cr -reactions investigation at 14.1 MeV neutron energy. Characteristics of these reactions have been calculated using TALYS code to estimate perspectives of using of this code in data interpretation in the TANGRA project. This project is performed in Frank Laboratory of Neutron Physics (FLNP JINR) to investigate properties of ($n,x\gamma$)-type reactions, important for fundamental and practical applications.

Keywords: Inelastic scattering, ^{24}Mg, ^{52}Cr, ^{12}C

1 Introduction

Reactions with fast neutrons are widely used in nuclear sciences. Investigation of the mechanism of these reactions could improve our knowledge on atomic nuclei structure. Information about these reactions is needed for fast neutron reactors and different kinds of industry devices developing[1]. One of the projects that studies the interaction of fast 14.1 MeV neutrons with various atomic nuclei is the TANGRA project[2,3], which is performed in the Frank Laboratory of Neutron Physics of the Joint Institute for Nuclear Research (JINR FLNP). The experimental setup used in this project provides possibility of the γ-quanta angular and energy distributions measurements. Search of the correct theoretical approach to calculate cross-sections and angular distributions of the γ-quanta emitted in ($n,x\gamma$)-type reactions is an important task of the TANGRA project. Due to the fact that TALYS 1.9 [2] is a quite universal program, which includes a number of theoretical models (optical model, DWBA, coupled-channel model, several models for level density). The usage of this program could be prospective with future modification to calculate the quantities, measured in our experiment. In this paper a comparison between calculation results and measured data for ^{12}C, ^{24}Mg and ^{52}Cr is presented to estimate the dynamics of discrepancy between calculation and experiment and to test the applicability of the TALYS program for data interpretation in the TANGRA project.

2 TANGRA Setup

The TANGRA setup consists of: portable tagged neutron generator ING-27, γ-ray detection system (Romashka, Romashka or HPGe) and data acquisition system (DAQ)[3]. Using of the tagged neutron method is an advantage of the experimental setup. This method is based on the fact that the neutron and the α-particle formed in the reaction:

$$d + t \rightarrow \alpha\left(3.5MeV\right) + n\left(14.1MeV\right) \quad \ldots (1)$$

in the laboratory frame are scattered in almost opposite directions. Therefore, knowing the direction of emission of α-particle, it is possible to recover the direction of the neutron, i.e. to "tag" it. In practice, the "tagging" of a neutron is done by using a position-sensitive (pixelated) alpha detector embedded in the neutron generator. Registration of α-particles permits to determine the intensity of the tagged neutron flux and realize α-γ (detectors) coincidence scheme. The tagged neutrons irradiate the target and induce

*Corresponding author (E-mail: na.fedorov@physics.msu.ru)

different nuclear reactions which could lead to γ–ray emission. The γ-quanta are registered in coincidence with α-particles. It has been shown[4] that using the $(\alpha - \gamma)$ coincidences helps to increase the signal-to-noise ratio and the accuracy of the experiment.

3 Neutron Scattering Cross-sections

3.1 Elastic scattering

Elastic neutron scattering is a process which doesn't change the internal energy of the target nucleus. There are two different mechanisms of this reaction: in the first case a compound nucleus is formed, in the second case this process takes place without compound nucleus formation: the scattering is going on the nuclear potential. For theoretical description of the direct scattering process an optical model is successfully used, for which individual parameters of the optical potential are needed for each nucleus. It is possible to estimate the optical potential using so called global parametrization which describes the dependence of optical parameters on A and Z (Ref. 5). For large range of nuclei so called best parameters are defined in TALYS by fitting parameters of optical potential. Cross sections of neutron elastic scattering σ_{el} are shown in Fig. 1 for ^{12}C, ^{24}Mg and ^{52}Cr. The calculation results are quite close to the experimental data[6–12] or ENDF/BVIII.0 estimations[13] for all used nuclei. However, the calculation doesn't reproduce the tiny structure of cross-sections energy dependence.

Angular distributions of elastic scattered neutrons ($(d\sigma/d\Omega)_{el}$) with energy close to 14.1 MeV are shown in Fig. 2. For ^{12}C calculations for E_n = 14.1 MeV neutrons coincide well with experimental data[9,14] for angles less than 90°. In the same time, the cross-sections for backscattering are underestimated. In case of ^{24}Mg, the calculations well describe the experiment[11] for angles <120°, for bigger angles θ the calculation result lies under the experimental data. We couldn't find data for elastic scattering of 14.1 MeV neutrons for ^{52}Cr so the calculation was made for 18.5 MeV neutrons and the results were compared with those from[15] (Fig. 2 c)), a good agreement was observed. We can deduce that the agreement between calculation and experiment becomes better with increasing of A, the impact of the compound processes in the same time decreases.

3.2 Inelastic scattering

The inelastic neutron scattering reactions always change the intrinsic energy of the target nucleus and they can go through compound or direct mechanism. For both of them data from optical model calculations are used. The energy dependences of inelastic scattering cross sections are shown in Fig. 3 σ_{inel} for ^{12}C, $J^{\pi} = 2^{+}$, 4.439MeV(a), for ^{24}Mg, $J^{\pi} = 2^{+}$,

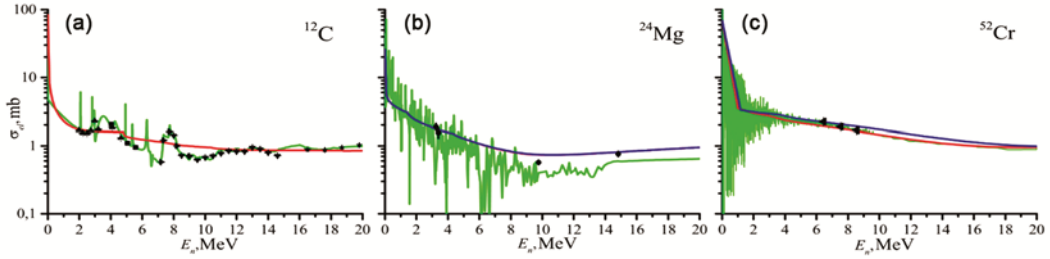

Fig. 1 — Dependence of the neutron elastic scattering on neutron energy σ_{el}: a – for ^{12}C (experimental data: Ref. 6-10), b – for ^{24}Mg (Ref. 11), c - for ^{52}Cr (Ref.12). Green line – ENDF/B-VIII.0 estimation(Ref. 13). Red line – TALYS 1.9 calculation with default parameters, blue line – calculation with "best parameters".

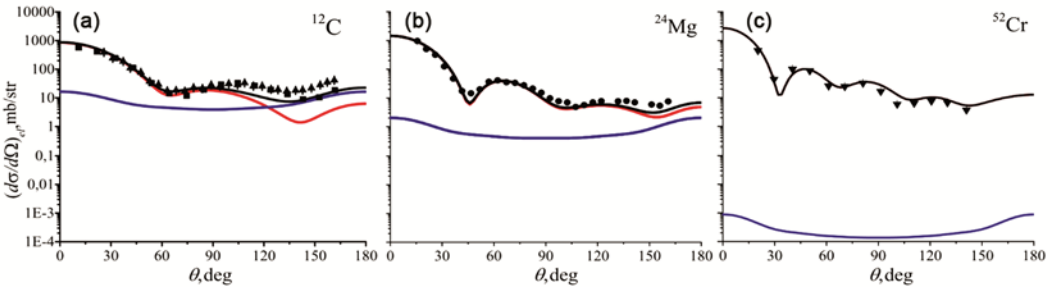

Fig. 2 — Angular distributions of scattered neutrons $(d\sigma/d\Omega)_{el}$, calculated with TALYS 1.9: a – for ^{12}C (squares – Ref. 9 (E_n = 14 MeV), triangles – Ref. 14 (14.43 MeV)), b – for ^{24}Mg (Ref. 11, 14.8 MeV), c – for ^{52}Cr (Ref. 15, 18.5 MeV). Blue line – share of compound processes, red line – direct processes, black line – sum.

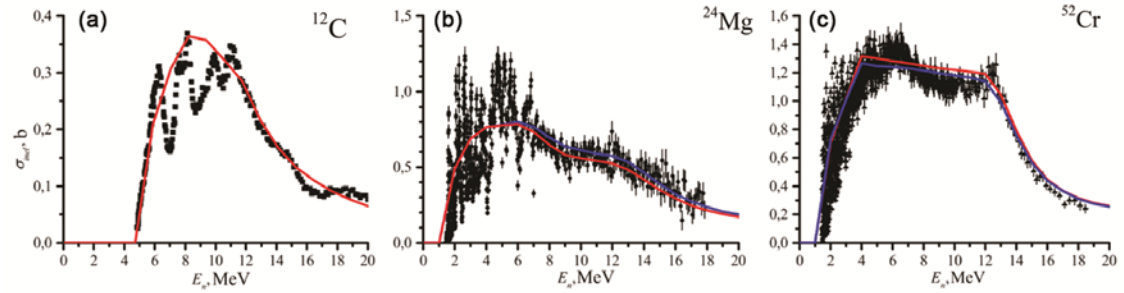

Fig. 3 — Dependence of σ_{inel} and σ_γ on E_n for first excited state of final nucleus: a – σ_{inel} for ^{12}C (experimental data– Ref.16), b – σ_γ for ^{24}Mg (Ref. 17), c – σ_γ for ^{52}Cr (Ref. 1). Red line – calculation result with default parameters, blue line – calculation with "best" parameters.

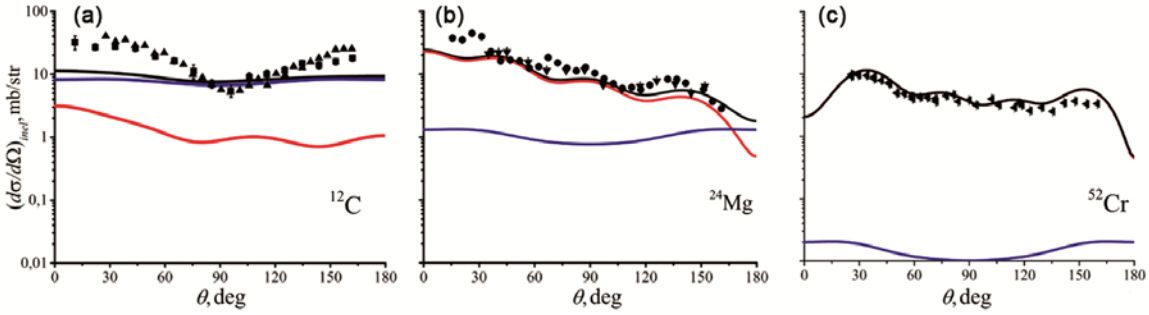

Fig. 4 — Angular distribution of inelastic scattered neutrons $(d\sigma/d\Omega)_{inel}$, calculated with TALYS 1.9: a – for ^{12}C (squares – Ref. 9, E_n = 14 MeV), triangles – Ref. 14,14.43 MeV), b – for ^{24}Mg (triangles – Ref. 18, 14.1 MeV), points–Ref. 11, 14.8 MeV), c – for ^{52}Cr (Ref. 19, 14.1 MeV). Blue line shows impact of the compound processes, red line – impact of the direct processes, black line – sum.

1.369 MeV (b) and for ^{52}Cr, $J^\pi = 2^+$ 1.434 MeV (c). The calculation results reproduce experimental data[1,16,17] good enough, but tiny structure still isn't described. Calculated angular distributions of the inelastic scattered neutrons $(d\sigma/d\Omega)_{inel}$ for first excited state of final nucleus are shown in the Fig. 4 for ^{12}C, ^{24}Mg and ^{52}Cr as well as shares of compound and direct components. Calculation results are quite close to the experimental values except for ^{12}C. For ^{12}C calculations significantly underestimate cross-sections for all angles except narrow area around 90º.

3.3 Gamma-ray emission cross-sections

The γ-ray emission cross-sections are important data for practical applications, they are needed for fast elemental analysis to estimate the elemental composition of irradiated sample. These cross-sections for ^{24}Mg and ^{52}Cr were measured, using HPGe γ–detector with TANGRA setup. We performed calculations of the γ-ray emission cross-sections using TALYS for ^{12}C, ^{24}Mg and ^{52}Cr. Calculated cross-section for 4.44MeV γ–line is 164 mb and this value could be overestimated because TALYS doesn't take into account the fact that higher excited states of ^{12}C decay through emission of α-particles. The amount of observed γ–lines in ^{24}Mg and ^{52}Cr is significantly higher because energy difference between neighbor levels decreases with growth of the nuclear mass.

In Table 1 a comparison between the calculations with TALYS 1.9, our results[20] and[21] is presented. The calculation results are quite close to the measured values except those for γ–transitions with E_γ = 3735.2 keV (the calculation result 2.1 times lower) and E_γ = 6246.8 keV (the calculation 1.6 times higher). In Table 2 results of the TALYS 1.9 calculations and experimental data for γ-transitions cross-sections observed from the irradiation of Cr with 14.1 MeV neutrons are shown. Comparison of measured values, obtained in the TANGRA experiment[22] with the calculation results demonstrates that TALYS 1.9 predictions are almost always lower than our experimental values. However, TALYS 1.9 calculations adequately coincide with experimental cross-sections; observed discrepancy for most intensive lines (E_γ = 935.5, 1333.6 and 1434.1 keV) are not higher than 18%. The significant difference between calculation and experiment for some low intensive lines may be connected with the insufficient accuracy of the branching ratios or with systematic experimental errors.

Table 1 — Observed γ–ray transitions for ^{24}Mg observed in TANGRA experiment [20]. Reactions lead to formation nuclei which emit γ–quanta as well as the spins and parities of initial $(J^{\pi})_i$and final $(J^{\pi})_f$states of γ–emitting nuclei listed in columns 3 and 4.

E_γ, keV	Reaction	$(J^{\pi})_i \rightarrow (J^{\pi})_f$	σ_γ, mb		
			TANGRA [20]	TALYS	[21]
350.7	^{24}Mg(n,α)^{21}Ne	$5/2_1^+ \rightarrow 3/2_{gs}^+$	185±2	123	77±13
440.0	^{24}Mg(n,d)^{23}Na	$5/2_1^+ \rightarrow 3/2_{gs}^+$	26±1.6	34	31±8
472.2	^{24}Mg(n,p)^{24}Na	$1_1^+ \rightarrow 4_{gs}^+$		153	126±20
1368.6	^{24}Mg(n,n')^{24}Mg	$2_1^+ \rightarrow 0_{gs}^+$	412	411	412±62
1809.0	^{26}Mg(n,n')^{26}Mg	$2_1^+ \rightarrow 0_{gs}^+$			82±13
2754.0	^{24}Mg(n,n')^{24}Mg	$4_1^+ \rightarrow 2_1^+$	55±3	82	55±11
3735.2	^{24}Mg(n,α)^{21}Ne	$5/2_1^+ \rightarrow 3/2_{gs}^+$	19±3	9	
3866.1	^{24}Mg(n,n')^{24}Mg	$3_1^+ \rightarrow 2_1^+$	25±3	34	33±5
4237.9	^{24}Mg(n,n')^{24}Mg	$2_2^+ \rightarrow 0_{gs}^+$	27±4	25	36±8
4642.2	^{24}Mg(n,n')^{24}Mg	$4_2^+ \rightarrow 2_1^+$	23±3	23	20±4
6246.8	^{24}Mg(n,n')^{24}Mg	$3_1^- \rightarrow 2_1^+$	13±3	21	24±4

Table 2 – The energy of gamma-rays and γ-production cross-sections for 52Cr, obtained in a TANGRA experiment [22], together with TALYS- calculations and those from other authors.

E_γ, keV [22]	E_γ, keV [13]	Reaction	σ_γ, mb				
			[22]	TALYS 1.9	[23]	[24]	[25]
126±3	124.45	^{52}Cr(n,p)^{52}V	28±2	7.6			
	125.08	^{52}Cr(n,p)^{52}V		14.4			
321±3	320.1	^{52}Cr(n,d)^{51}V	25±3	10.3			14±1
648±3	647.47	^{52}Cr(n,n')^{52}Cr	77±3	12.2			70±4
747±3	744.23	^{52}Cr(n,n')^{52}Cr	92±3	63.5		128±21	71±4
	749.07	^{52}Cr($n,2n$)^{51}Cr		45,5			42±1
937±3	935.54	^{52}Cr(n,n')^{52}Cr	254±4	236.9	221±31	211±26	237±9
1249±3	1246.28	^{52}Cr(n,n')^{52}Cr	46±3	21.87			48±8
1335±3	1333.65	^{52}Cr(n,n')^{52}Cr	200±4	163.1	239±36	173±29	205±8
1436±3	1434.07	^{52}Cr(n,n')^{52}Cr	785±6	761.5	757±56	738±51	783±30
1533±3	1530.67	^{52}Cr($n,2n$)^{51}Cr	54±5	32.9		74±23	
1728±3	1727.53	^{52}Cr(n,n')^{52}Cr	39±3	18.9			26±4
2040±5	2038	^{52}Cr(n,n')^{52}Cr	18±3	11.8			
2339±5	2337.44	^{52}Cr(n,n')^{52}Cr	14±3	20.1			

4 Conclusions

TALYS 1.9 – is a complex program for nuclear reaction calculation with large quantity of adjustable parameters. The calculated cross-sections for nuclei considered in this work are quite close to the experimental data. It is important to notice that the agreement between calculation and experimental data becomes better with increasing of the nuclear mass. Probably this fact is connected with features of the global parameterization of the optical model. We couldn't reproduce the angular distribution of the inelastic scattered neutrons, using TALYS 1.9, for the first excited state at 4.44 MeV of ^{12}C. Moreover, it is not possible to calculate the angular distribution of the γ-quanta, emitted by residual nucleus after nucleon emission, so, we have to modify TALYS code for further usage in the TANGRA project.

References

1 Mihailescu L C, Borcea C, Koning A J & Plompen A J M, *Nucl Phys A*, 786 (2007) 1.

2 Alexakhin V Y, Bystritsky V M, Zamyatin N I, Zubarev E V, Krasnoperov A V, Rapatsky V L, Rogov Yu N, Sadovsky A B,

Salamatin A V, SalminRA, Sapozhnikov M G, Slepnev V M, Khabarov S V, Razinkov E A, Tarasov O G & Nikitin G M, *Nucl Instrum Meth A*,785 (2015) 9.

3 Ruskov I N, Kopatch Y N, Bystritsky V M, Skoy V R, Shvetsov V N, Hambsch F J, Oberstedt S, Capote N R, Sedyshev P V, Grozdanov D N, Ivanov I Z, Aleksakhin V Y, Bogolubov E P, Barmakov Y N, Khabarov S V, Krasnoperov A V, Krylov A R, Obhodaš J, Pikelner L B, Rapatskiy V L, Rogachev A V, Rogov Y N, Ryzhkov V I, Sadovsky A B, Salmin R A, Sapozhnikov M G, Slepnev V M, Sudac D, Tarasov O G, Valković V, Yurkov D I, Zamyatin N I, Zeynalov S S, Zontikov A O & Zubarev E V, *Phys Proc*, 64 (2015) 163.

4 Bystritsky V M, Zamyatin N I, Zubarev E V, Rapatsky V L, Rogov Y N, Romanov I V, Sadovsky A B, Salamatin A V, Sapozhnikov M G, Safonov M V, Slepnev V M & Filippov A V, *Phys Part Nucl Lett*, 10 (2013) 442.

5 Koning A J & Delaroche J P, *Nucl Phys A*, 713 (2003) 231.

6 Boschung P, Lindow J T & Shrader E F, Nucl Phys A, 161 (1971) 593.

7 Velkley D E, Brandenberger J D, Glasgow D W, McEllistrem M T, Manthuruthil J C & Poirier C P, *Phys Rev C*, 7 (1973) 1736.

8 Demanins F, Granata L, Nardelli G & Pauli G, *Lettereal Nuovo Cimento*, 8 (1973) 259.

9 Haouat G, Lachkar J, Sigaud J, Patin Y & Coçu F, *Nucl Sci Eng*, 65 (1978) 331.

10 Olsson N, Trostell B & Ramstrom E, *Nucl Phys A*, 513 (1990) 205.

11 Haouat G, Lagrange C & Patin Y, *Proc Conf Nucl Data Sci Technol*, Springer Netherlands, (1983) 796.

12 Kinney W E & Perey F G, Oak Ridge National Laboratory Report No 4806. (1974).

13 Evaluated Nuclear Structure Database ENSDF: https:// www.nndc.bnl.gov/ensdf/

14 Glasgow D W, Purser F O & Hogue H, *Nucl Sci Eng*, 61 (1976) 521.

15 Yamanouti Y, Sugimoto M, Chiba S, Mizumoto M & Hasegawa K, *Proc Conf Nucl Data Sci Technol*, Springer-Verlag Berlin Heidelberg, (1992) 717.

16 Rogers V C, Orphan V J, Hoot C G & Verbinski V V, *Nucl Sci Eng*, 58 (1975) 298.

17 Olacel A, Borcea C, Dessagne P, Kerveno M, Negret A & Plompen A J M, *Phys Rev C*, 90 (2014) 034603.

18 Clarke R L & Cross W G, *Nucl Phys*, 53 (1964) 177.

19 Schmidt D & Mannhart W, *Phys Technol Bundesanst Neutronen Phys Rep*, 31 (1998).

20 Fedorov N A, Grozdanov D N, Kopatch Y N, Bystritsky V M, Tretyakova T Y, Ruskov I N, Skoy V R, Dabylova S, Aliev F A, Hramco C, Gundorin N A, Dashkov I D, Bogolyubov E P, Yurkov D I,Gandhi A & Kumar A, *Bull Russ Acad Sci Phys*,(2020). (in press).

21 Nyberg-Ponnert K, Jonsson B & Bergqvist I, *Phys Scr*, 4 (1971) 165.

22 Grozdanov D N, Fedorov N A, Kopatch Y N, Bystritsky V M, Tretyakova T Y, Ruskov I N, SkoyV R, Dabylova S, Aliev F A, Hramco C, Gundorin N A, Dashkov I D, Bogolyubov E P, Yurkov D I, Gandhi A & Kumar A, *Phys Atom Nucl*, (2020). (in press).

23 Abbondanno U, Giacomich R, Lagonegro M & Pauli G, *J Nucl Energy*, 27 (1973) 227.

24 Yamamoto T, Hino Y, Itagaki S & Sugiyama K, *J Nucl Sci Techol*, 15 (1978) 797.

25 Oblozinsky P, Hlavac S, Maino G & Mengoni A, *Il Nuovo Cimento A,* 105 (1992) 965.